Available online at www.sciencedirect.com

ScienceDirect

Procedia Engineering 213 (2018) 173–182

Procedia Engineering

www.elsevier.com/locate/procedia

7th International Conference on Fatigue Design, Fatigue Design 2017, 29-30 November 2017, Senlis, France

Toward composite wind turbine blade fatigue life assessment using ply scale damage model

Damien CAOUS[a,b,]*, Christophe BOIS[c], Jean-Christophe WAHL[c], Thierry PALIN-LUC[b], Julien VALETTE[a,c]

[a]*TENSYL, 48 rue Jacques de Vaucanson, Pôle Arts&Métiers, 17180 Périgny, France*
[b]*Arts et Métiers ParisTech, I2M, CNRS, Esplanade des Arts et Métiers, 33405 Talence, France*
[c]*Université de Bordeaux, I2M CNRS, 15 rue de Naudet, 33170 Gradignan, France*

Abstract

Fatigue design optimization of composite material structures is limited by the classical approaches used, derived from knowledge based on metal fatigue. Other approaches exist to describe damage mechanisms of composites but they cannot always be applied at the structure scale because of their complexity. However, assumptions can be made in the case of beam structures to reduce the structural investigation at the section scale. With these assumptions this paper proposes to compare a progressive fatigue damage model written at the ply scale to the normative approach for the assessment of wind turbine blade section design. It is shown that the normative approach is very conservative and the progressive fatigue damage model provides very useful information to understand damage propagation at the structure scale.

Peer-review under responsibility of the scientific committee of the 7th International Conference on Fatigue Design.

Keywords: Damage model, Fatigue, Wind turbine blade

1. Introduction

At the present time, the wind power industry is facing the double challenge of further increasing the size of turbines for off-shore production and making them lighter for land-based production, so that they can be adapted for

* Corresponding author. Tel.: +33 (0)5 46 28 22 83
E-mail address: damien.caous@tensyl.com

1877-7058
Peer-review under responsibility of the scientific committee of the 7th International Conference on Fatigue Design.
10.1016/j.proeng.2018.02.019

use in less windy areas. The main stumbling block has been identified in the hope that the design of the blades can be optimised to meet these challenges, and it concerns the precision of their design under fatigue.

A wind turbine blade is generally designed to be in rotational operation for 20 years in wind fields that by their very nature are variable. This creates structures that are highly subject to fatigue. We are talking about 10^8 cycles approximately, which makes fatigue over a long lifetime the main design criterion [1]. In addition to high resistance to fatigue, the material used for the blades should have a low mass, which has a direct impact on stress, sufficient stiffness so that it does not impair the aerodynamic properties of the turbine, and a cost that makes wind energy competitive. With all these elements combined, it soon became clear that glass fibre non-crimp fabrics (NCF), with possibly carbon fibres locally with polyester or epoxy matrices, were required for medium and large sized blades. Although long fibre composites have high resistance to fatigue, there is as yet no commonly accepted design method devoted specifically to these materials and the normative approach currently used in the context of blade certification is based on a transposition of existing knowledge of the fatigue behaviour of metals [2]. In this study, the normative approach is compared with a progressive fatigue damage model written at the ply scale.

2. Calculation methods

2.1. Calculating stresses at the section scale

Stresses in the blade are traditionally calculated section by section based on assumptions of the behaviour of beam structures. First, it is assumed that the blade sections remain flat and perpendicular to the neutral fibre (Euler Bernoulli beam theory). From this, we formulate a relation between longitudinal strain ε_x on the laminates in the section, under tensile loading and bending, and strain in the section expressed in the form of axial strain a (in mm/mm) and bending strains (b, c) (in mm^{-1}):

$$\varepsilon_x = a + b.x_B + c.y_B \tag{1}$$

where x is the longitudinal axis of the laminate which coincides with the longitudinal axis of the blade z_B. x_B and y_B are the coordinates of the laminated element of the section within the blade coordinate system (x_B, y_B, z_B) (Fig. 1.a).

Assuming that the laminates are subjected to in-plane stress state ($\sigma_z = 0$), membranous (constant strain in the thicknesses of the laminates), and where $\sigma_y = 0$, it can be shown that for a section formed of balanced laminates its bending-traction behaviour can be expressed in the form:

$$\begin{Bmatrix} F_{zB} \\ M_{yB} \\ M_{xB} \end{Bmatrix} = \begin{bmatrix} <EA> & <Em_X> & <Em_Y> \\ -<Em_X> & -<EI_{YY}> & -<EI_{XY}> \\ <Em_Y> & <EI_{XY}> & <EI_{XX}> \end{bmatrix} \begin{Bmatrix} a \\ b \\ c \end{Bmatrix} \tag{2}$$

where $<EA>$, $<Em_X>$, $<Em_Y>$, $<EI_{XX}>$, $<EI_{YY}>$ and $<EI_{XY}>$ are the terms for the stiffness matrix of the section [3].

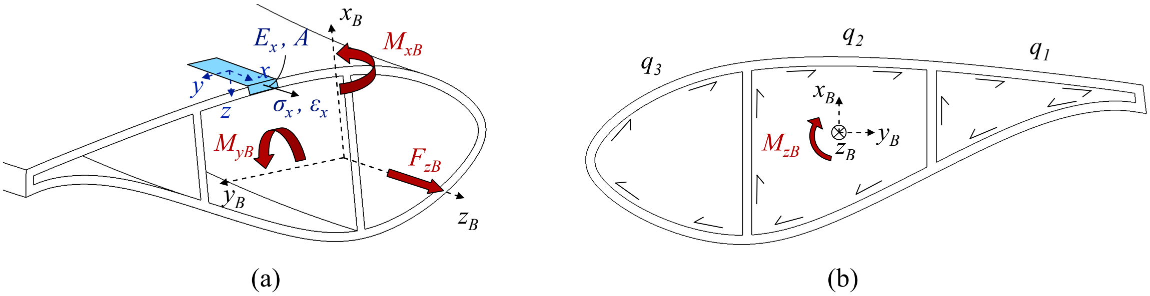

Fig. 1. (a) Markers and notations to describe a blade section under bending and traction
(b) Shear flow in a section of wind turbine blade made up of 3 closed cells

By disregarding the transverse loads, the shear flow in the section, shaped by balanced laminates, is linked with the torsional load on the blade (Fig. 1.b). Assuming that shear flow qi is constant in each cell of the section, which can be assumed for thin composite skins, it can be shown that the shear flow for each cell is proportional to the rotation ψ (in rad/mm) of the section:

$$\underline{q} = 2\,[\delta]^{-1}\,\underline{\Omega}\,\psi \tag{3}$$

where $\underline{\Omega}$ is the sector area of the section and $\underline{\underline{\delta}}$ is the matrix defined by the following equations [4]:

$$\delta_{ii} = \oint_i \frac{ds}{Gh} \qquad and \qquad \delta_{ij} = \delta_{ji} = -\int_{i,j} \frac{ds}{Gh} \tag{4}$$

Finally, by the integral of the shear flow across the section, we obtain:

$$M_{zB} = 4\underline{\Omega}^T\,[\delta]^{-1}\,\underline{\Omega}\,\psi \tag{5}$$

Note that when the laminates in the section are not balanced or are damaged in an asymmetrical way, coupling between the longitudinal and shear behaviour of the laminates leads to a coupling between the traction-bending behaviour and the behaviour under torsion at the section scale. This is expressed in a behaviour equation as follows:

$$\begin{Bmatrix} F_{zB} \\ M_{yB} \\ M_{xB} \\ M_{zB} \end{Bmatrix} = [K] \begin{Bmatrix} a \\ b \\ c \\ \psi \end{Bmatrix} \tag{6}$$

where the coupling terms of the stiffness matrix *[K]* are non-zero terms.

Note that with these assumptions, the strain state of each laminate in the section is known from its behaviour and the displacement of the section (a,b,c,ψ). This displacement is known for a torsor of internal forces (F_{zB}, M_{yB}, M_{xB}, M_{zB}) at the section scale. Stresses at the ply level or laminate level are then obtained from the behaviour of each of them, based on their strains.

2.2. Fatigue design using the normative approach

The normative approach described here is based on the recommendations of the DNV-GL certification body [5]. A flow diagram of this approach is given in Fig.2.a. Before analysing the blade under fatigue, a representative annual loading sequence must first be defined for the turbine by calculating loads. This is done by carrying out a dynamic simulation of the whole turbine under wind and operating conditions supplied by the certification bodies. The loads applied to the blades are of different origins: aerodynamic pressure of the wind on the external surface, gyration stresses, gravity, stresses related to the turbine control; and they generate a multiaxial and non-proportional loading at the scale of the structure [6]. Therefore the cycles counting cannot be based on the history of the load at the structure scale. It has to be based at the laminate scale.

The history of the longitudinal stresses is therefore calculated at the scale of the laminates in the section according to the method described above. Cycles are counted for each laminate element in the section using the Rainflow method. This method identifies cycles of stresses of constant amplitude from their average stress $\sigma_x^{m,i}$ and their amplitude $\sigma_x^{a,i}$ in the loading sequence, and their occurrence n^i over the time period considered.

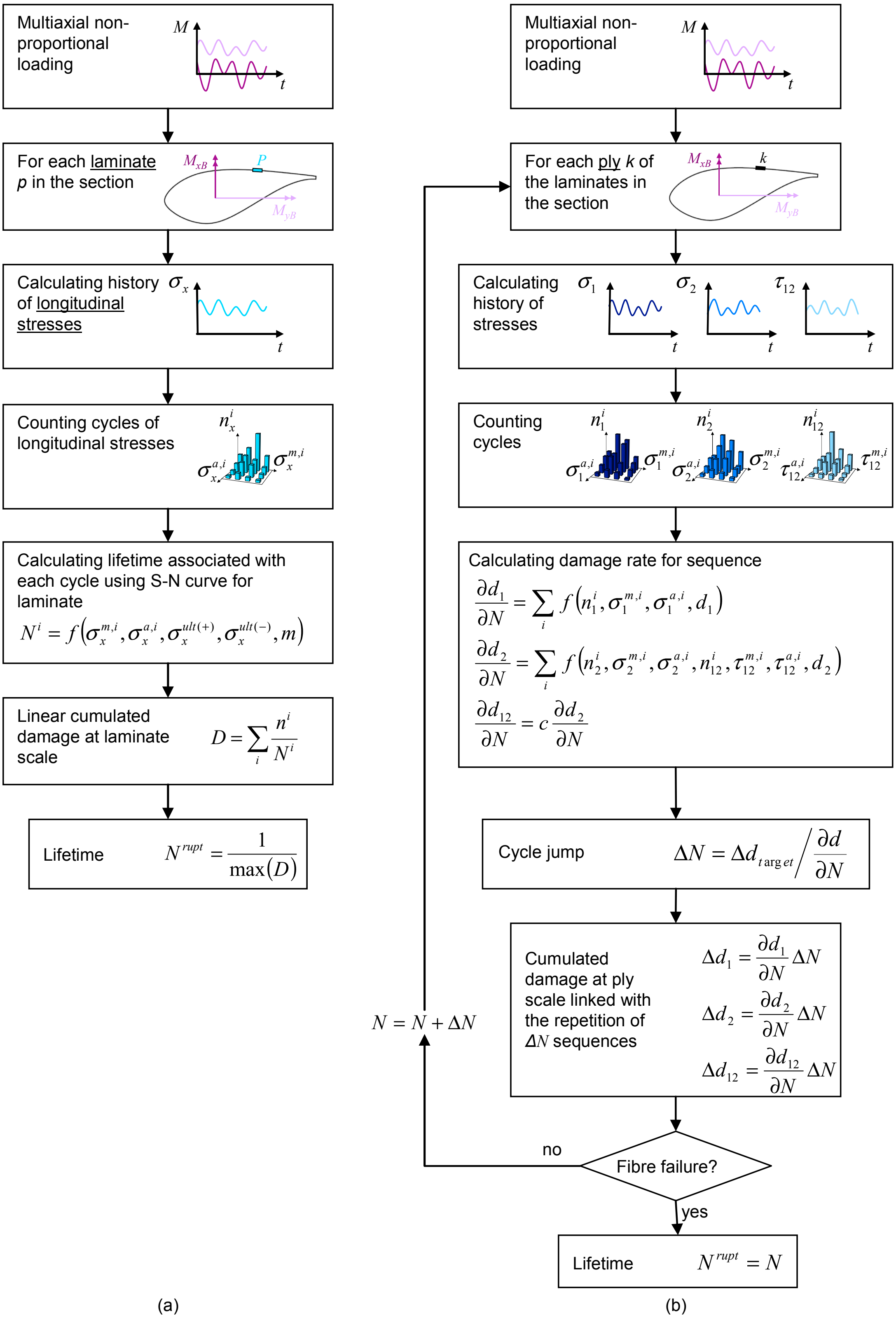

Fig. 2. Diagram showing (a) the linear normative approach, (b) the progressive damage model

A lifetime N^i is associated to each cycle identified by the counting method, using the S-N curve for the laminate. The S-N curve for the load ratio of the cycle is generated from failure stresses in traction $\sigma_x^{ult(+)}$ and in compression $\sigma_x^{ult(-)}$ and also from a slope parameter m according to the following equation:

$$N^i = \left[\frac{\sigma_x^{ult(+)} + \left|\sigma_x^{ult(-)}\right| - \left|2.\sigma_x^{m,i} - \sigma_x^{ult(+)} + \left|\sigma_x^{ult(-)}\right|\right|}{2.\sigma_x^{a,i}} \right]^m \tag{7}$$

Here it is important to understand that the slope parameter m is the same for all the laminates. In addition, stresses at failure are calculated using the lamination theory, with the mechanical characteristics of the UD ply, based on the failure criterion of the first ply.

The accumulated total damage at the laminate scale, across all the cycles identified during counting, is done linearly, according to Miner's rule:

$$D = \sum_i \frac{n^i}{N^i} \tag{8}$$

A damage value $D = 1$ is associated to laminate failure. Maximum damage $\max(D)$ to the section laminates is selected for the simulated loading sequence. The number of repetitions in the sequence before failure, or the lifetime of the blade if the loading sequence is representative of a year of operation, is obtained from:

$$N^{rupt} = \frac{1}{\max(D)} \tag{9}$$

2.3. Fatigue design using a progressive damage model

The normative approach proposes a linear calculation of damage. In other words, damage is calculated for a loading sequence, then by assuming that repeating this sequence produces the same damage, the lifetime is obtained for damage $D = 1$.

In contrast, fatigue design using a progressive damage model takes into account damage associated with preceding loading sequences when calculating the damage of the current loading sequence. An iterative calculation is therefore performed until laminate failure is detected (Fig. 2.b). The cycle jump approach was selected (Fig. 3.).

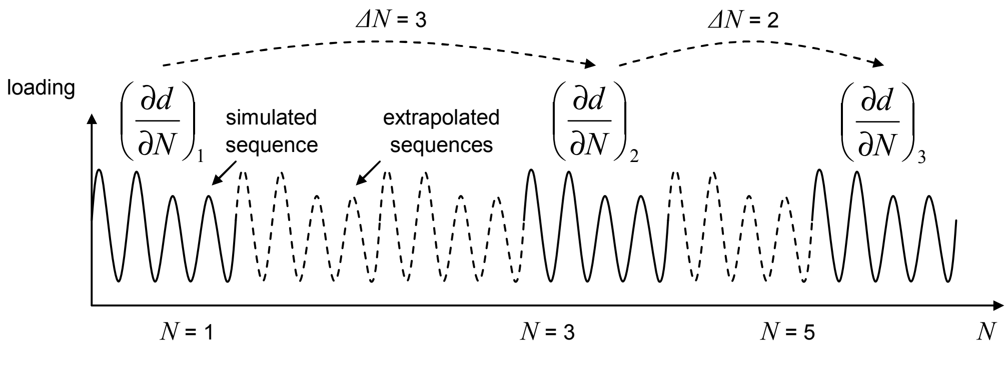

Fig. 3. Illustration of the principle of the cycle jump [7]

The damage model considered [8]–[10] was formulated at the ply scale and was inspired by studies by Christian Hochard's team [11]–[13]. Internal damage variables (d_1, d_2, d_{12}) describe loss of stiffness under cumulated static-fatigue loading in each direction:

$$\begin{cases} E_1 = E_1^0(1-d_1) & \\ E_2 = E_2^0 & \text{for } \sigma_2 < 0 \\ E_2 = E_2^0(1-d_2) & \text{for } \sigma_2 \geq 0 \\ G_{12} = G_{12}^0(1-d_{12}) & \end{cases} \tag{10}$$

where E_1, E_2, G_{12}, E_1^0, E_2^0 and G_{12}^0 denote the actual and initial modules in the directions of the fibre, transverse in the plane and shear respectively. Using a fourth internal variable at the ply scale the residual strain can be modelled so that it is correlated in shear and transverse direction.

The change in loss of stiffness under fatigue is driven by the amplitude and the maximum thermodynamic force associated to each damage variable:

$$\frac{\partial d_1}{\partial N} = a_1(1-d_1)^{\gamma_1}\left(Y_{d_1^f}\right)^{l_1}\left(\Delta Y_{d_1^f}\right)^{l_2} \tag{11}$$

$$\frac{\partial d_2}{\partial N} = a_2(1-d_2)^{\gamma_2}\left(Y_{d_2^f}\right)^{m_1}\left(\Delta Y_{d_2^f}\right)^{m_2} + b_2(1-d_2)^{\gamma_2}\left(Y_{d_{12}^f}\right)^{n_1}\left(\Delta Y_{d_{12}^f}\right)^{n_2} \tag{12}$$

$$\frac{\partial d_{12}}{\partial N} = c\frac{\partial d_2}{\partial N} \tag{13}$$

where a_1, a_2, b_2, c, γ_1, γ_2, l_1, l_2, m_1, m_2, n_1 and n_2 are material parameters to be identified, N is the number of cycles, and $Y_{d_i^f}$ and $\Delta Y_{d_i^f}$ are defined by the following relations:

$$Y_{d_1^f} = \frac{\sigma_1^{\max 2}}{2E_1^0(1-d_1)^2}, \quad Y_{d_2^f} = \frac{\langle\sigma_2^{\max}\rangle_+^2}{2E_2^0(1-d_2)^2} \quad \text{and} \quad Y_{d_{12}^f} = \frac{\tau_{12}^{\max 2}}{2G_{12}^0(1-d_{12})^2} \tag{14}$$

$$\Delta Y_{d_1^f} = \frac{(\sigma_1^{\max}-\sigma_1^{\min})^2}{2E_1^0(1-d_1)^2}, \quad \Delta Y_{d_2^f} = \frac{\left(\langle\sigma_2^{\max}\rangle_+ - \langle\sigma_2^{\min}\rangle_+\right)^2}{2E_2^0(1-d_2)^2} \quad \text{and} \quad \Delta Y_{d_{12}^f} = \frac{(\tau_{12}^{\max}-\tau_{12}^{\min})^2}{2G_{12}^0(1-d_{12})^2} \tag{15}$$

The drop in stiffness in the direction of the fibre is very limited for a large part of the loading then becomes fast a few cycles before failure (Fig. 4.a) while the loss of transverse and shear stiffness is progressive under fatigue (Fig. 4.b).

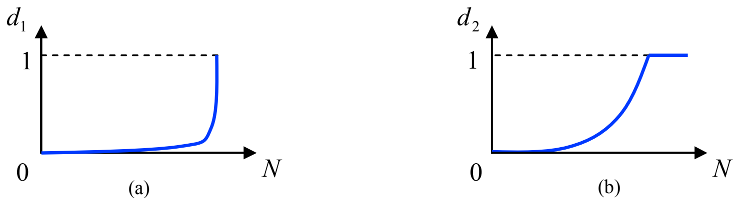

Fig. 4. Representation of damage evolution laws under fatigue, (a) fibre direction, (b) matrix

For each loading sequence, the history of plane stresses (σ_1, σ_2, τ_{12}) is calculated in each ply of the laminate elements in the section based on the assumptions made in paragraph 2.1 and taking into account the damage, associated with the preceding sequences, to all the laminates that make up the section. The cycles were counted based on stresses at the ply scale, component by component, then the damage rate linked with the sequence was calculated, first in the fibre direction and then in the matrix, from equations (Eq. 11) to (Eq. 13) by summing the damage rate for each cycle identified by the counting method. The matrix damage rate is therefore composed of a linear combination of a transverse damage rate and the shearing damage rate (Eq. 12). Once the damage rate in each direction of each ply for all the laminate elements of the section is known, damage is extrapolated over *ΔN* sequences by the cycle jump approach. The value of cycle jump *ΔN* is adapted to the damage rate using the method described by Paepegem [7]. This method involves setting a target damage increment Δd_{target} and calculating the cycle jump needed to achieve this damage in each direction of each ply.

$$\Delta N = \Delta d_{target} \Big/ \frac{\partial d}{\partial N} \tag{16}$$

The final cycle jump *ΔN* considered for the complete section is selected by considering the frequency distribution of the cycle jumps needed to achieve Δd_{target} in each ply. The damage increment for the cycle jump is then obtained explicitly in each ply of the laminate elements in the section:

$$\Delta d_1 = \frac{\partial d_1}{\partial N}\Delta N, \ \Delta d_2 = \frac{\partial d_2}{\partial N}\Delta N, \ \Delta d_{12} = \frac{\partial d_{12}}{\partial N}\Delta N \tag{17}$$

Finally, if a failure is detected along the fibre direction (dependent for each ply on the maximum stress in the fibre direction, fatigue damage in the fibre direction and matrix damage [10], [13]) the sum of the cycle jumps completed up to that point gives the number of sequence repetitions, or the lifetime if the sequence is representative of a year of operation by the structure. If not, a new iteration is carried out by calculating the damage for the same sequence but updating the damage to the section. This damage can affect stress distribution due to change in stiffness and hence it can also affect the change in damage during fatigue loading. However, this change in stiffness is not used to update the loading sequence calculated when the loads are calculated. Note that the cycles may be interrupted at any point in the calculation in order to obtain the damage state of the section at the end of a selected operating time.

3. Comparison of the two approaches

3.1. Material scale

We specified above that the slope parameter *m* of the S-N curves used for the normative approach was the same as for the laminates as a whole. This parameter, traditionally identified using the S-N curve of a 0°, is generally taken as being equal to 10. A comparison of S-N curves at $R = 0.1$ is shown in Fig. 5 for a glass-epoxy [0] laminate and a [±45/0/±45] laminate. In this second laminate, ply thickness at 0° represents 23% of total thickness. The S-N curves for the two approaches are compared with tests on specimens prepared by infusion.

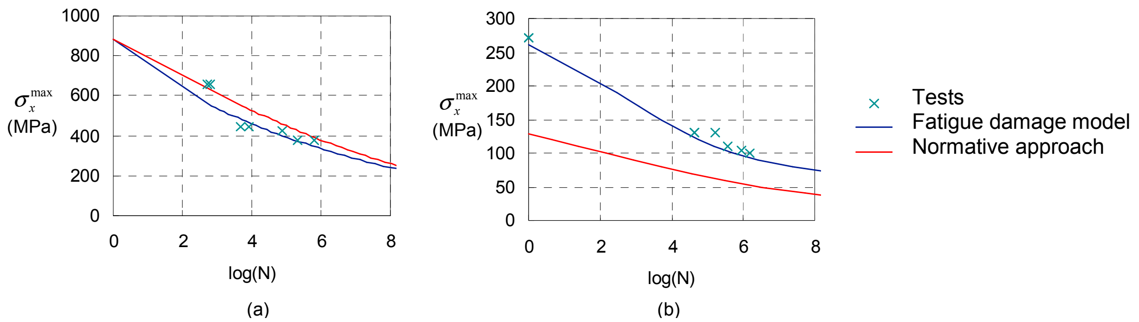

Fig. 5. Comparison of S-N curves at R = 0.1 (a) of a [0] at V_f = 50% and (b) of a [±45/0/±45] at V_f = 40%

We observe that the choice of parameter $m = 10$ gives an S-N curve for the normative approach at $R = 0.1$ which is close to the test results for 0°. Concerning the [±45/0/±45] laminate, note that the stress at static failure is very much underestimated. This is due to the first ply failure criterion which forecast off-axis ply failure early in the loading. The S-N curve of the laminate based on this static failure stress (Eq. 7) is therefore also conservative.

3.2. Structure scale

3.2.1. Case study

Let us consider fatigue damage to a 23 m blade, in normal shut down conditions in normal wind conditions. The average wind speed considered at hub height, $z_{hub} = 46$ m, is equal to the wind at which the turbine stops: $V_{hub} = 25$ m/s. In these conditions the turbine rotates at 23 rpm before shutting down. This is not a case of critical loading of the blade and the loads obtained provide very long fatigue life which is outside the validity domain of the model used. Therefore, loads were multiplied by a factor 10 in order to get results that can be analyzed. The components of the torsor of internal forces, in the blade coordinate system (Fig. 1), at 8.8 m span is given in Fig. 6 after having been multiplied by a factor 10.

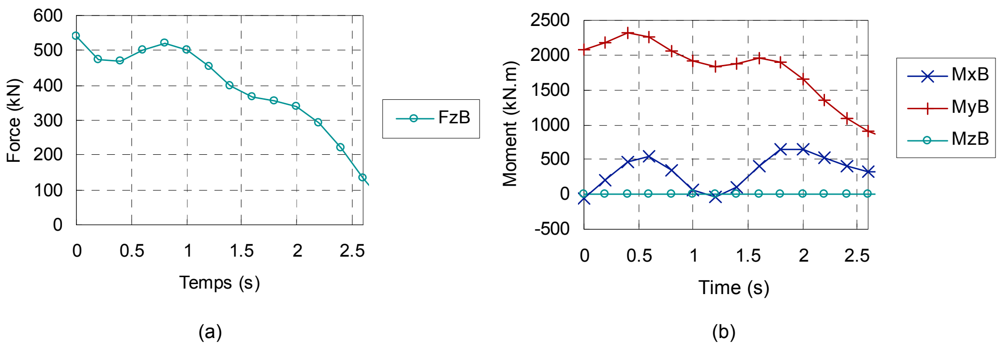

Fig. 6. (a) Forces and (b) internal moments multiplied by a factor 10 at 8.8 m span of blade G1 for a wind turbine normal shut down in normal wind conditions for $V_{hub} = 25$ m/s

The blade section considered here consists of [±45] composite skins over the entire section. Reinforcements at 0° are introduced at the leading edge, the trailing edge and on either side of the profile in the maximum thickness area in order to recover the bending loads. This area is called the spar cap and is the main blade stiffener which enables the bending moments associated with aerodynamic forces to be recovered.

3.2.2. Fatigue damage model results

The progressive fatigue damage model provides the stiffness loss in each ply of the blade section during the fatigue life until a ply fails in the fibre direction. When fibre failure is detected ($d_1 = 1$) in one ply, the section is considered failed and the fatigue life is obtained.

The fatigue damage model, provide a failure of a ply in the fibre direction in the spar-cap area on the pressure side of the blade at $4{,}6.10^5$ cycles (Fig. 7.b.). At failure, the matrix damage in ±45° plies has reached the maximum value for a lot of laminates of the pressure side (Fig. 7.a.). Indeed, the fatigue damage model considered, allows matrix damage and takes into account the fatigue damage to forecast ply failure in the fibre direction.

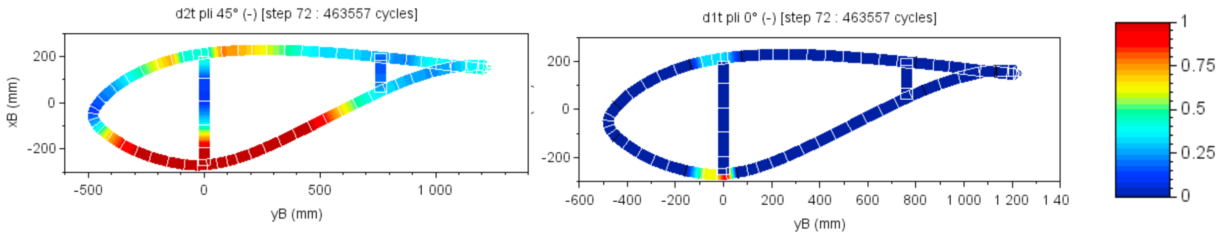

(a) (b)

Fig. 7. (a) Matrix damage d_2 in +45° plies of the 8.8 m span of blade G1 (b) Fibre damage d_1 in 0° plies of the 8.8 m span of blade G1

3.2.3. Comparison of the two approaches

The fatigue damage model gives a lot of information that the normative approach cannot give. For example: stiffness losses (at the ply scale but also at the section scale), residual strength and residual strains. The comparison of the two approaches at the blade scale will be made on the only result given by the normative approach: the fatigue life. It is shown in Fig. 8, which displays the fatigue life obtained with both approaches as a function of the factor applied on the loads, that the normative approach provides a failure of the section for a loading factor 3.7 times lower that the one that provide failure with the progressive fatigue damage model for the same fatigue life: 4,6.10^5 cycles.

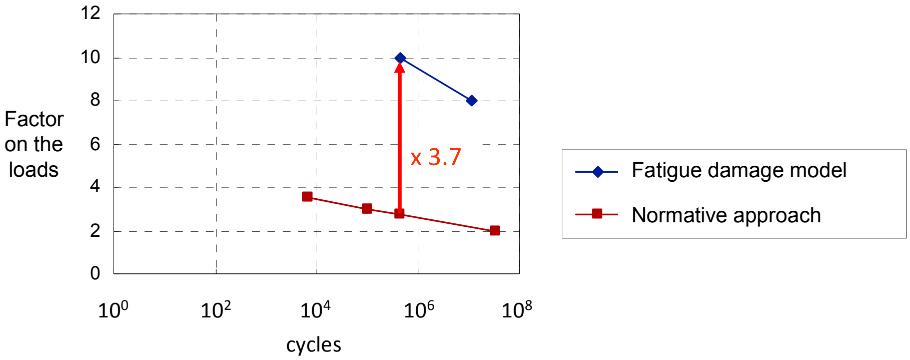

Fig. 8. Comparison of the two approaches in terms of fatigue life of the 8.8 m span of blade G1 as a function of the factor applied on the loads

4. Conclusion

After a brief presentation of the normative approach and a fatigue damage model at ply scale, they were compared to evaluate fatigue damage in a section of a wind turbine blade under cyclic loading. It appears that the normative approach is highly conservative. This seems to be related to the assumptions made to generate the S-N curves of the laminates which were based on determining the failure stress of the laminate from the mechanical characteristics of the plies using the laminate theory, based on a failure criterion with maximum stress in the first ply. In addition, the normative approach is linear and therefore gives the zone in which the damage is initiated but cannot predict how it will evolve. The damage model, however, describes the evolution of the damage. It identifies the zone in which the damage is initiated, and then gives the change in damage over the entire section until failure of the UD plies in the fibre direction. First, this gives a lifetime that corresponds to destruction of the structure rather than to first damage that is generally not critical. Next, with the information from the damage model it is possible to monitor the state of health of the structure during its operational phase and anticipate maintenance interventions. In terms of future prospects, note that this case study does not describe loading of the section over the complete operational phase of the turbine and a more representative example should be simulated. In particular, this would show the advantage of the damage model for complex loading sequences.

Acknowledgements

The blade studied in this article was designed by the TENSYL company as part of the EFFIWIND project, founded by the Nouvelle Aquitaine Region and ADEME.

References

[1] J. F. Mandell, R. M. Reed, and D. D. Samborsky, "Fatigue of Fiberglass Wind Turbine Blade Materials", Sandia National Laboratories, United States, Sandia Report SAN92-7005, 1992.
[2] T. Burton, N. Jenkins, D. Sharpe, and E. Bossanyi, *Wind Energy Handbook*, Second Edition. Wiley, 2011.
[3] R. M. Rivello, "Bending and Extension of Beams", in *Theory and Analysis of Flight Structures*, McGraw-Hill, 1969, p. 133‑177.
[4] L. Wang, X. Liu, L. Guo, N. Renevier, and M. Stables, "A mathematical model for calculating cross-sectional properties of modern wind turbine composite blades", *Renewable Energy*, vol. 64, p. 52‑60, April 2014.
[5] Germanischer Lloyd, "Guideline for the certification of Wind Turbines", Germanischer Lloyd, 2010.
[6] D. Caous, C. Bois, J.C. Wahl, T. Palin-Luc, and J. Valette, "Analysis of multiaxial cyclic stress state in a wind turbine blade", presented at the 20th International Conference on Composite Materials (ICCM20), Copenhagen, Denmark, 2015.
[7] W. Van Paepegem, J. Degrieck, and P. De Baets, "Finite element approach for modelling fatigue damage in fibre-reinforced composite materials", *Composites Part B: Engineering*, vol. 32, no. 7, p. 575‑588, Oct. 2001.
[8] D. Caous, C. Bois, J.C. Wahl, T. Palin-Luc, and J. Valette, "Construction et identification d’un méso-modèle pour la prédiction de la durée de vie et la résistance résiduelle des composites stratifiés", presented at the SF2M 36èmes Journées de Printemps, Paris, France, 2017.
[9] D. Caous, "Rôle de l’endommagement sur la durée de vie en fatigue des matériaux composites stratifiés : application au domaine éolien", PhD, Arts et Métiers ParisTech, France, publication in 2017.
[10] D. Caous, C. Bois, J.-C. Wahl, T. Palin-Luc, and J. Valette, "A method to determine composite material residual tensile strength in the fibre direction as a function of the matrix damage state after fatigue loading", *Compos Part B: Eng*, vol. 127, p. 15-25, October 2017.
[11] J. Payan, "Etude du comportement de composites stratifiés sous chargement statique et de fatigue", PhD, Université Aix-Marseille II, France, 2004.
[12] Y. Thollon, "Analyse du comportement à rupture de composites stratifiés constitués de plis tissés sous chargements statique et de fatigue", PhD, Université Aix-Marseille II, France, 2009.
[13] C. Hochard, S. Miot, and Y. Thollon, "Fatigue of laminated composite structures with stress concentrations", *Composites Part B: Engineering*, vol. 65, p. 11‑16, Oct. 2014.